Fractal approach of turbulent dispersion

J.M. Redondo[1,2]

[1] Dept. Física Aplicada, Universitat Politécnica de Catalunya
B5 Campus Nord UPC, Barcelona 08034, Spain

[2] D.A.M.T.P., University of Cambridge, Wimberforce Av. Cambridge,
England. United Kingdom.

1. Introduction

There are several techniques suitable for measuring and modelling dispersion from scalar or velocity-field measurements in a turbulent flow. Each of these has peculiar features and sometimes, even different scaling, and a careful choice has to be made depending on the kind of information available and needed. A useful way to investigate diffusion is to make use of the fractal and multifractal information that ocean and atmospheric flows provide. Here we present some fractal based techniques, where the velocity and scalar fields are related to the spectral spatial information that they provide and are used to predict diffusivity and mixing.In addition an Eulerian description can be obtained by interpolation from Lagrangian information, which is much easier to model via Kinematic Simulation or synthetic turbulence type models, because the detail velocity field is eventually sampled in a random statistical way in the whole domain during their time evolution. It is not possible to get reliable Lagrangian information using PIV since the transformation from the Eulerian description to the Lagrangian one implies an integration in time of the velocity field, especially when considering phenomena that show high sensitivity to initial conditions (turbulent flows). We show some examples of oil spill dispersion in the ocean surface and discuss several multifractal and scaling approaches.

2. Fractal Methods and KS turbulence models

Fractal objects, as they are called, display self-similarity over a range. The Hausdorff dimension can be used to describe them for physical objects. In general, there is a limited range where self-similarity applies. In turbulence this range is found between the largest scale and the Kolomogorow scale. A practical definition of the fractal dimension, D_i can be given as

$$D_i = \frac{\log N}{\log\left(\frac{1}{\sigma}\right)}$$

where N is the number of self-similar parts or covering boxes at size σ. An extension of the fractal dimension to a set where different isolines have different fractal dimensions may be done using multifractals. For a fractal curve, its measured length L will have a power law dependence on the measuring yardstick as: $L \propto \sigma^{1-D_i}$. The exponent D_i is called the fractal dimension of the curve and is a measure of the roughness of fragmentation of the curve and have the subindex i represents the Euclidean dimension of the embedding space $i = \{1,2,3,.....n\}$. The fractal convolutions of turbulent interfaces will increase the area between different marked regions of the flow. In similar way as above we can express the area determined by the fractal set as $A \infty \sigma^{2-D_2}$, if the range of scales where self-similarity is exhibited is limited by, say, a large scale l

and a small scale, say the Kolomogorow length scale η_k, then the increase in area of a turbulent interface due to the fractal behaviour, which at scales comparable to *l* measures A_l, is

$$A_l \left(\left(\frac{l}{\eta} \right)^{2-D_2} - 1 \right)$$

This increase in contact area needs to be taken into account when mixing through density interfaces is discussed. This geometrical descriptor is useful in different circumstances as higher fractal dimensions generally indicate more flow convolutions. Multifractal analysis will aid in the parameterizations of the different mixing efficiencies produced by the different basic instabilities.

This characterization of multifractal measures is the concept of generalized dimensions D_q, which corresponds to the scaling exponents for the qth moment of the measure (different to the embeding space, as above) defined as:

$$D_q = \lim_{\delta \to 0} \frac{1}{1-q} \frac{\log \sum_{i=1}^{n(\delta)} m_i^{\,q}}{\log \delta}$$

The singularity index (α) can be determined by Legendre transformation of the $\tau(q)$ curve as:

$$< \alpha(q) > = \frac{d < \tau(q) >}{dq}$$

The number of cells of size δ with the same α, $n_\alpha(\delta)$, is related to the cell size as $n_\alpha(\delta) \propto \delta^{-f(\alpha)}$, where $f(\alpha)$ is a scaling exponent of the cells with common α. Parameter $f(\alpha)$ can be related to the evolution of the Fractal dimension with any mass (image or scalar) related function. It is nevertheless important to note the differences between very similar box/counting methods, when the chosen limits or pracical fit intervals used when calculating *D(q)* are used.

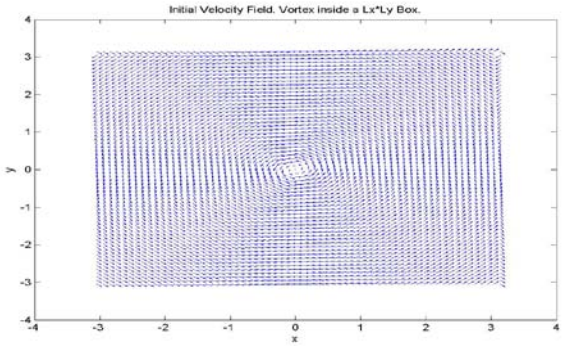

Fig. 1. Simple Model of background of a large single eddy induced mean velocity used in the KS models of dispersion.

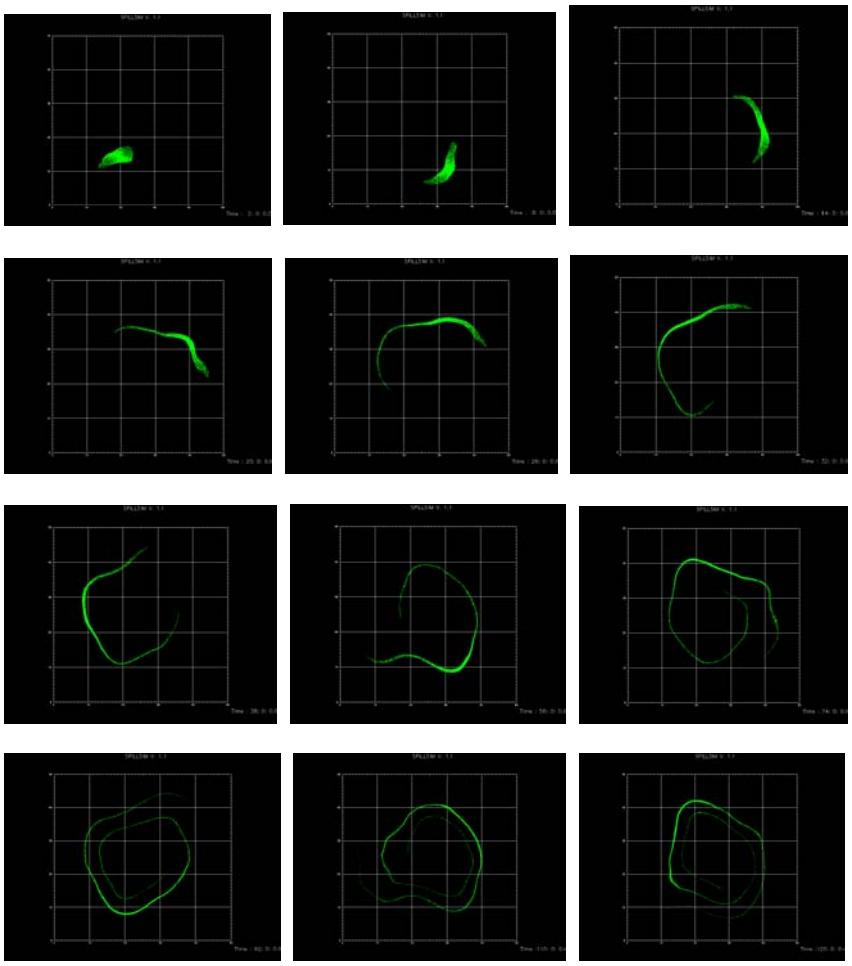

Fig. 2. Dispersion in a turbulent environment KS simulation of a simulated oil spill in the ocean surface, the turbulence intensity is low I=0.5.

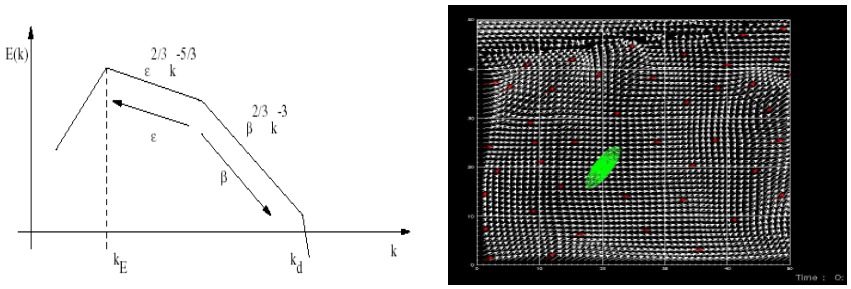

Fig. 3. 2D model spectral conditions used in the KS simulation, (right) Feebback of data on the time evolution of the KS velocity field.

The Kinematic Simulation model used, described in Castilla(2000, 2001) similar to that used by Fung et al.(1992) and Malik et al.(1993,1999) has been used to compare measured diffusion with different levels of overall turbulent intensity I = u'/U, with the added possibility of modifying the whole spectral signature, whose integral contributes to the (u') turbulent energy. A result that may be

difectly applied to ocean oil spills is to relate the growth of the maximum fractal dimension of a spill in time to the residence time (Redondo et al. 2008,2009).
The understanding of transport and mixing properties of passive impurities, or in general of tracers in fluid flows is of great practical importance in several fields of environmental sciences and engineering. The method of particle tracking or buoy tracking in the ocean, seeding particles (or buoys or balloons in the Ocean and Atmosphere) and then following them during their motion within the measured domain or volume is able to return a very usefull set of Lagrangian velocity samples are associated with fluid particles rather than merely with a location, i.e. in a Lagrangian reference frame. Pollutant dispersion is an example of a phenomenon naturally described in the Lagrangian frame of reference. In fact, pollutants act as tracers of fluid particles, thus it is convenient to describe the behaviour of the fluid particles once they are released from the source, as they move within the field, we will asume that the scalar tracers follow in a passive way the velocity field, and discuss their spatial scaling. If we introduce a scaling factor λ raised to the scaling exponent H (that we call the Hölder factor or the Hurst exponent) in the velocity field we can study the behaviour of the system under the following transformations arising from a simple change in scale

$$v \to \lambda^H v',\ t \to \lambda^{1-H} T',\ r \to \lambda r',\ p \to \lambda^{2H} p',\ F \to \lambda^{2H-1} F'$$

We can see that, if we consider $\nu = 0$, the scaling of coordinates in an inviscid flow (Euler's equation) leads to:

$\lambda^{2H-1}\left[\partial_T v + v\nabla v + \nabla p\right] = 0$ so we may model turbulent viscosity as either A) $\nu \to \lambda^{H+1}\nu$: the viscosity scales with other variables, which is good for LES models or as. B) $\nu = const$: the viscosity remains constant at every scale, good for a DNS type model. Working hypothesis A) satisfies the scale invariance for every value of H, while hypothesis B) holds only for $H = -1$.
In figures 2, 4 and 6, we may observe the very different topological characteristics of natural sliks and oil spills. In figure 10, advanced flow visualization techniques aid the identification of vortices or of Langmuir cells. The different causes of the slicks are also reflected in the *D(r)* plots discussed above and used first by Gade and Redondo (1999). Other multifractal measurements can also be related to physical mechanisms that affect in a different fashion the different scalar intensities used to identify the flows, as in Castilla(2000) and Redondo(1990) where stratification is shown to affect clearly the maximum fractal dimension.

The correlations of intensity values and the radial integral of these, indicates the spatial scale *l* where the SAR intensities are well correlated. If we suppose that the surface currents are responsible (at least partly) for the spatial distribution of the ocean roughness for two main reasons, first the slope at both sides of an eddy is very different at producing radar backscatter from a side (as happens with ERS-1/2 and also ENVISAT and RADARSAT), This length scale in environmental flows is closely related to the Rossby deformation radius (Platonov et al 2008, 2009), and may be used to evaluate diffusivity.

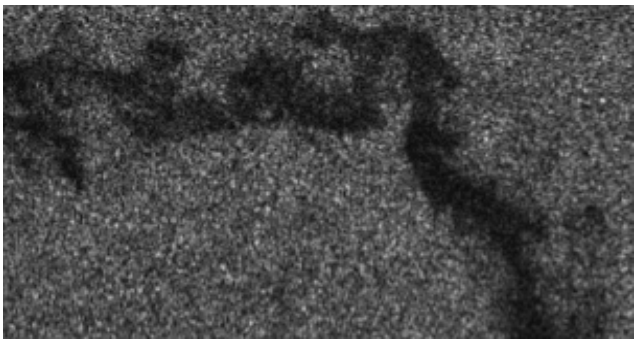

Figure 4. ASAR higher resolution image of a wethered oil spill..

For example, the oil spill shown in figure 4, at a higher resolution using ASAR would correspond to a range of non- dimensional times T_{oil} between 0.7 and 0.8 matching the fractal dimension of 1.3-1.4. There are other indications that may be useful from the SAR observations, such as the low local wind at the time the image was taken. There is a consistent pattern that distinguishes the recent oil spills and the natural slicks that have adapted to the multi-scale turbulent flow of the ocean surface. Figure 5 is similar to the last image of figure 2, but the local turbulent intensity is higher, (with a spectral signature as that shown in figure 3) thus it is easily seen that the convolution are greater and the fractal dimension is higher.

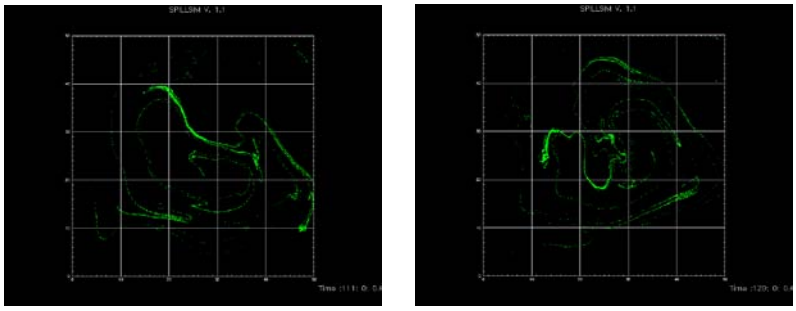

Fig. 5. Dispersion in a turbulent environment KS simulation

4. Results and Discussion

Experimental observations of SAR features are investigated with multi-scale fractal techniques in order to extract relevant information on the spectral characteristics of mixing and diffusive events. Both density and tracer marked oil spills and slicks are investigated in detail using third order structure function analysis that indicates strong inverse cascades towards the large scales producing spectral variations

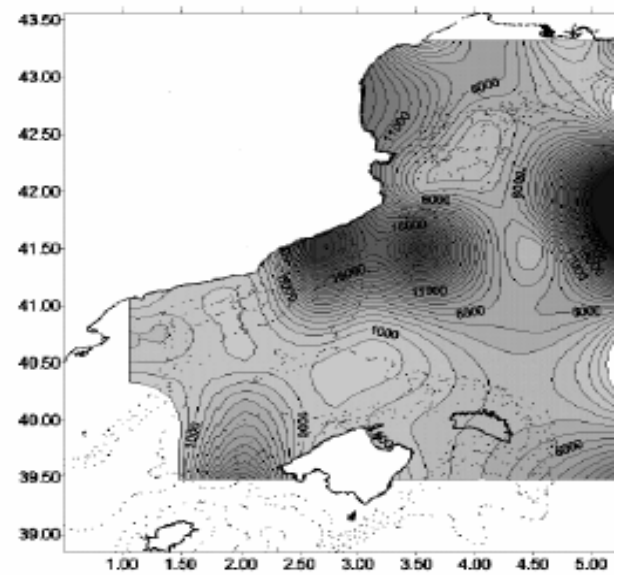

Fig. 6. . 2D map of Eddy diffusivity values derived from local estimates of the integral scale from SAR images.

If we want to apply these scaling to, say the vortex size evolution, it would be interesting to compare the spectra with the Hurst exponent of second order. We know (Tarquis et al. 2009) that if $H(2)=\frac{1}{3}$, (Kolmogorov, 3D scaling) then the power exponent is $p=5/3$ in a similar way for Kraichnan´s 2D enstrophy cascade region where $p=3$ then $H_{2D}(2)=1$.If we use the maximum fractal dimension like Redondo (1990, 1996) then from $p=2E_u+1-2D_{E_u}$, so for 3D flows $p=7-2D_3$ and for 2D flows $p=5-2D_2$. So if $p=5/3$ in a fully 3D flow $D_3=2.66$ and if $p=3$ then $D_2=1$. If a Kolomogorov spectra appears in a 2D flow then $D_2=1.66$. Both types of flows can co-exist both in the Atmosphere and the Ocean as indicated by Platonov et al. (2008). The role of intermittency would give other values. Several uses of these new techniques are proposed taking advantage of Zipf's Law, both for anthropogenic oil spills and other features, it is possible to predict the likely probability of oil spill accidents of different sizes, as well as the local eddy characteristics that strongly influence the turbulent horizontal diffusivity, *K(x,y).*As an example from [6], figure 14 shows a map of local average diffusivities derived from SAR observations near Barcelona, of course Richardson's law has to be applied and different sizes of spills will comply with the 4/3 law. Both numerical simulations [4] and laboratory experiments confirm the conditions for hyperdiffusion ($D^2 = c\, t^{n(f,N)}$ with $n(f,N) > 3$) to exist, as well as the trapping associated with coherent structures and vortices. Figure 6 is an eddy diffusivity map derived from SAR measurements of the ocean surface, using the Rossby deformation radius obtained loccally by performing a feature spatial correlation of the available images of the region. Both the multifractal discrimination of the local features and the diffusivity measurements are important to evaluate the state of the environment.

References

Artale V., Boffetta G., Celani A., Cencini M. and Vulpiani A.(1997)Dispersion of passive tracers in closed basins beyond the diffusion coefficient,Physics of Fluids, 9, 3162

Boffetta G. and Celani A. (2000) Pair dispersion in turbulence, Physica A, 280, 1-9

Boffetta G., Lacorata G., Redaelli G. and Vulpiani A., (2001)Detecting barriers to transport: a review of diferent techniques, Physica D, 159, 58-70.

Castilla, R. (2000). Numerical simulations of particles diffusion in isotropic and homogenous turbulent flows. In Redondo, J. and Babiano, A., editors, Turbulent Diffusion in the Environment, pages 69–76, Barcelona. Xarxa Tematica de Dinamica de Fluids i Turbulencia Geofisica.

Castilla, R. (2001) Ph.D. thesis, ETSCCPB. Univ. Politecnica de Catalunya.

Deardoff J.W. and Willis G.E., (1985) Further results from a laboratory model of the convective planetary boundary layer", Bound.-Layer Meteorol., 32, 205-36

Fung, J. C. H., Hunt, J. C. D., Malik, N. A., and Perkins, R. J.(1992). Kinematic simulation of homogeneous turbulence by unsteady random fourier modes. J. Fluid Mech.236. Gade M. and Redondo J.M. (1999) Marine pollution in European coastal waters monitored by the ERS-2 SAR: a comprehensive statistical analysis. IGARSS 99. Hamburg. v. III, 1637-1639. 308-312.

Hanna S.R., (1981) Lagrangian and Eulerian time scale relations in the day-time boundary layer", J. appl. Met., 20, 242-249.

Malik N.A., Dracos T. and Papantoniou D.A. (1993) Particle tracking velocimetry in three-dimensional flow", Exp. in Fluids, 15, 279-294.

Monin A.S. and Yaglom A.M., (1971) Statistical fluid mechanics: mechanics of turbulence, The MIT press, Cambridge, Massachusetts, 1, 769.

Malik, N. A. and Vassilicos, J. C. (1999). A lagrangian model for turbulent dispersion with turbulent-like flow structure: Comparison with direct numerical simulation for twoparticle statistics. Physics of Fluids, 11(6), 1572–1580.

Monin, A. S. and Ozmidov, R.V. (1985). Turbulence in the Ocean. D. Reidel Publ. NY.

Platonov A, A. Tarquis, E. Sekula and J. M. Redondo, “SAR observations of vertical structures and turbulence in the ocean ”, MODELS, EXPERIMENTS AND COMPUTATION IN TURBULENCE, R. Castilla, E. Oñate and J.M. Redondo (Eds.), CIMNE, Barcelona 2007.

Redondo J.M., A. Matulka, A. Carrillo and R. Castilla. “Turbulent difusión in strongly stratified and rotating flows” Topics in Fluid Dynamics, (Ed. Prihoda I and Kozel K.) 124-129. CAS, Prague.

Redondo J.M. and Platonov A “Aplicacion de las imagines SAR en el studio de la dinamica de las agues y de la polucion del mar Mediterraneo cerca de Barcelona”. Ingenieria del agua, 8 (1), 15-23. 2001.

Redondo J.M. “Fractal models of density interfaces”. Wavelets, Fractals and Fourier transforms. (Eds.) M. Farge, J.C.R. Hunt and J.C. Vassilicos. 353-370. IMA number 43, Clarendon Press, Oxford 1993.